Available online at www.sciencedirect.com
SCIENCE DIRECT®
Physics Letters B 625 (2005) 203–211
PHYSICS LETTERS B
www.elsevier.com/locate/physletb

First observation of very neutron-deficient ^{122}Ce

J.F. Smith [a], C.J. Chiara [b,c], M.P. Carpenter [d], H.J. Chantler [e], P.T.W. Choy [e], C.N. Davids [d], M. Devlin [c,f], J.L. Durell [a], D.B. Fossan [b], S.J. Freeman [a], R.V.F. Janssens [d], N.S. Kelsall [g], T. Koike [b], D.R. LaFosse [b], E.S. Paul [e], P. Reiter [d], D.G. Sarantites [c], D. Seweryniak [d], K. Starosta [b,h], R. Wadsworth [g], A.N. Wilson [g,1], P.-H. Heenen [i]

[a] *Schuster Laboratory, University of Manchester, Manchester M13 9PL, United Kingdom*
[b] *Department of Physics and Astronomy, State University of New York at Stony Brook, Stony Brook, NY 11794-3800, USA*
[c] *Department of Chemistry, Washington University, St. Louis, MO 63130, USA*
[d] *Argonne National Laboratory, Argonne, IL 60439, USA*
[e] *Oliver Lodge Laboratory, University of Liverpool, Liverpool L69 7ZE, United Kingdom*
[f] *LANSCE-3, Los Alamos National Laboratory, Los Alamos, NM 87545, USA*
[g] *Department of Physics, University of York, Heslington, York YO10 5DD, United Kingdom*
[h] *National Superconducting Cyclotron Laboratory and Department of Physics and Astronomy, Michigan State University, East Lansing, MI 48854, USA*
[i] *Service de Physique Nucléaire Théorique, Université Libre de Bruxelles, CP 229, 1050 Bruxelles, Belgium*

Received 22 April 2005; received in revised form 28 June 2005; accepted 10 August 2005

Available online 22 August 2005

Editor: V. Metag

Abstract

Excited states have been identified in the very neutron-deficient ^{122}Ce nucleus. This is the first observation of this nucleus and its excited states. The ground-state rotational band has been observed up to spin 14 $\hbar$. The band has been assigned to ^{122}Ce by detecting gamma rays in coincidence with evaporated charged particles and neutrons. The $E(2_1^+)$ value suggests a rather large ground-state deformation of $\beta_2 = 0.35$, in good agreement with Hartree–Fock–Bogoliubov (HFB) mean-field calculations. The aligned angular momentum of the band has been studied and is compared with those of the neighboring even–even cerium isotopes, and to Woods–Saxon cranking calculations. The non-observation of the $\pi(h_{11/2})^2$ alignment until at least 0.4 MeV/$\hbar$ is consistent with the extracted value of β_2.

PACS: 21.10.Re; 23.20.Lv; 27.60.+j; 29.30.Kv

E-mail address: john.f.smith@manchester.ac.uk (J.F. Smith).
[1] Present address: Australian National University, Canberra ACT 0200, Australia.

0370-2693/$ – see front matter
doi:10.1016/j.physletb.2005.08.035

The physics of nuclei with a large excess of neutrons or protons has become one of the focal points of nuclear-structure research. Calculations have suggested that the properties of these *exotic* nuclei differ significantly from those of near-stable nuclei [1]. The cerium ($Z = 58$) isotope chain presents good candidates in which to probe the structure of nuclei with extreme neutron deficiency. The light cerium isotopes are known to be well deformed in their ground states [2–4], with quadrupole deformation parameters $\beta_2 \simeq 0.3$. For the isotopes with neutron number $64 \leqslant N \leqslant 74$, the proton Fermi level lies in the prolate-driving, low-Ω $h_{11/2}$ orbitals, and the neutron Fermi level is located higher in the $h_{11/2}$ sub-shell. As N decreases below about 74, the neutrons become progressively more prolate driving, increasing the ground-state deformation. This trend is supported by theoretical calculations [5,6] which predict that the deformation will reach a maximum for $N = 64$, ^{122}Ce. Also, in these nuclei, cranked-shell-model calculations predict that the rotational alignments of pairs of both neutrons and protons from the $h_{11/2}$ sub-shell will take place at low rotational frequencies. The precise rotational frequency at which these alignments occur depends sensitively on the deformation; thus, an experimental study of the alignments can reveal information about global nuclear-structure properties.

The cerium isotopes with $A \geqslant 125$ have all been comprehensively studied; details are given in Refs. [3,4,7–9]. The isotope ^{124}Ce has been investigated several times by in-beam gamma-ray spectroscopy: most recently, the ground-state band was delineated up to 30 $\hbar$ [3]. The isotope ^{123}Ce has been identified [10], but to date, no excited states have been reported. The isotope ^{122}Ce lies very close to the proton dripline. Some recent calculations have predicted that ^{122}Ce itself may decay by the emission of alpha-particles and exotic clusters [11,12], although these are not predominant decay modes. Prior to this work, no experimental information was available *at all* for this nucleus. One of the primary reasons why the cerium isotopes with $A < 124$ have not been studied is that they are difficult to produce in experiments. The best way to produce them is to use heavy-ion fusion–evaporation reactions, but the isotopes with $A < 126$ can only be reached by neutron evaporation from compound nuclei which are themselves very neutron deficient. Consequently, the production cross sections are very small; charged-particle evaporation dominates the total cross section. In the present work, an experiment has been carried out with the Gammasphere gamma-ray spectrometer [13], in order to identify the low-lying excited states of ^{122}Ce. Seven E2 transitions, have been assigned to the ground-state rotational band, which extends up to 14 $\hbar$.

Excited states in ^{122}Ce were populated using the ^{64}Zn(^{64}Zn, $\alpha 2n$) reaction, for which the cross section, predicted by the statistical-model code ALICE [14], is several hundred μb. The 2-pnA ^{64}Zn beam was accelerated to 260 MeV by the ATLAS accelerator system at Argonne National Laboratory. The beam was incident upon a target consisting of a 500-μg/cm^2 ^{64}Zn foil. The Gammasphere spectrometer [13] was used to detect gamma rays emitted at the reaction site. In normal operation, Gammasphere consists of 110 75%-efficient high-purity germanium detectors, arranged in 17 rings of constant polar angle, θ. In the present work, the forward-most five rings of germanium detectors were removed in order to accommodate the Washington University Neutron Shell [15], leaving 78 germanium detectors in Gammasphere. The Neutron Shell consists of 30 BC501A scintillators, and was used to detect evaporated neutrons. The Microball charged-particle spectrometer [16] of 95 CsI(Tl) scintillators was also utilized in the experiment to detect evaporated alpha particles and protons. After the target, recoiling reaction products were dispersed according to their mass-to-charge state (M/q) ratio by the Argonne Fragment Mass Analyzer (FMA) [17], and were detected in a parallel-plate gridded-anode avalanche counter (PGAC) at the focal plane. Data were recorded when any one of three trigger conditions was satisfied: $\gamma\gamma\gamma$ (Gammasphere only); $\gamma\gamma$-neutron; or $\gamma\gamma$-recoil.

The experiment lasted for about 84 hours, during which time 1.04×10^9 events were written to magnetic tape. The coincidence data had a mean suppressed gamma-ray fold of 2.8. Much of the offline analysis was carried out with two- and three-fold gamma-ray coincidence events, known as *doubles* and *triples*. As a starting point in the analysis, two-dimensional histograms, or *matrices*, and a three-dimensional histogram, or *cube*, were created from the unfolded doubles and triples; each n-fold event was unfolded into ${}^nC_2$ doubles and ${}^nC_3$ triples, resulting in a total of 7.0×10^9 doubles and 2.7×10^9 triples. The spec-

tra were analyzed using the RADWARE data analysis codes ESCL8R and LEVIT8R [18]. Analysis of the cube revealed that excited states were populated in at least 20 evaporation residues, with the most intense being ^{125}La ($3p$), ^{122}Ba ($\alpha 2p$), and ^{124}Ba ($4p$), which constituted 26%, 21%, and 10% of the data, respectively.

Discrimination between alpha particles and protons in the Microball was carried out using the methods described in Ref. [16]. Similarly, discrimination between gamma rays and neutrons in the Neutron Shell was carried out using the methods described in Ref. [15]. In the Microball, the detection efficiencies were found to be $\sim 84\%$ for protons and $\sim 69\%$ for alpha particles. The detection efficiency for neutrons in the Neutron Shell was not easy to determine for several reasons. First, one of the three triggers used in the experiment included the detection of a neutron ($\gamma\gamma$-neutron), and the data were therefore biased. Any measured efficiency can only be considered as an *effective* efficiency. Second, the detection efficiency depends on the energy of the evaporated neutron [15], and is dependent upon the reaction channel. And third, a significant proportion of neutrons are observed to scatter between detectors. This has the effect of reducing the neutron-detection efficiency and of 'contaminating' gated spectra with gamma rays from channels of lower neutron multiplicity. In order to reduce the effects of scattering, a method of *nearest-neighbor suppression* was used as described in Refs. [15,19,20]. This suppression affected the single-neutron detection efficiency ε_n, and meant that the efficiency for the detection of two neutrons ε_{2n} was not simply ε_n^2. Ultimately, *effective* efficiencies of $\varepsilon_n \simeq 55\%$ and $\varepsilon_{2n} \simeq 9\%$ were obtained.

In order to search for gamma-ray transitions in ^{122}Ce, matrices were created which were gated by all combinations of particles that were likely to be evaporated during the reaction, and by different M/q values. This resulted in a total of about 30 matrices. Inspection of the matrix gated on $\alpha 2n$ (leading to ^{122}Ce) revealed intense gamma-ray transitions with energies of 136, 298, 437, and 557 keV which were candidates for the ground-state band of ^{122}Ce. Gating on these transitions revealed them to be in coincidence with each other, and also with transitions at 658, 744, and tentatively 812 keV. Before these transitions could be unambiguously assigned to ^{122}Ce, several other possible assignments had to be discounted. It is possible, for example, that the transitions belong to a reaction channel with higher particle multiplicity, such as $2\alpha 2n$, $\alpha p 2n$, or $\alpha 3n$, and that one or more of the particles has escaped detection, or that they belong to a channel in which a single neutron is evaporated, and that the neutron has scattered from one neutron detector to another. Inspection of the $\alpha p 2n$-, $2\alpha 2n$-, and $\alpha 3n$-gated matrices shows no evidence of these gamma rays, which rules out the evaporation of any protons or more than one α particle or more than two neutrons. Usually, the best way to distinguish between the αn, $\alpha 2n$, and $\alpha 3n$ reaction channels would be to use the data from the PGAC at the focal plane of the FMA. The excellent M/q resolution allows spectra to be created which are effectively gated on evaporation residues with different masses. Unfortunately, however, the large range of recoil angles inherent to α-particle-evaporation channels meant that the transport efficiency of the FMA for ^{122}Ce was found to be about 2%. Thus it was not possible to use the FMA data for very low-intensity reaction products.

This analysis, therefore, leaves the possibility of the candidate gamma rays belonging to the αn or $\alpha 3n$ reaction channels, on an $\alpha 2n$ channel from a target contaminant. The evaporation of αn will leave the residue ^{123}Ce. Prior to this experiment there were no known excited states in ^{123}Ce, but in the present data, several cascades of gamma rays have been assigned to this nucleus; this will be reported in a separate paper [20]. The assignment to the $\alpha 3n$ channel is discounted for several reasons. First, an inspection of the $\alpha 3n$-gated matrix does not show evidence for the candidate transitions with intensities that would be expected from the measured detection efficiencies. Second, no other three-neutron evaporation channels have been observed in this reaction, or in similar reactions [21,22]. And third, the predicted $\alpha 3n$ cross section [14] is about 50 nb.

The isotopic origin of the gamma rays can be investigated by measuring their intensities in the various particle-gated matrices. If the candidate ^{122}Ce band does indeed belong to the $\alpha 2n$ evaporation channel, then it should be present not only in the $\alpha 2n$-gated matrix, but also in matrices gated on lower evaporated-particle multiplicities; specifically αn, α, $2n$, and n, and on events with nothing detected by the Microball and the Neutron Shell. The intensity of the candidate ^{122}Ce band was determined in each of these matrices

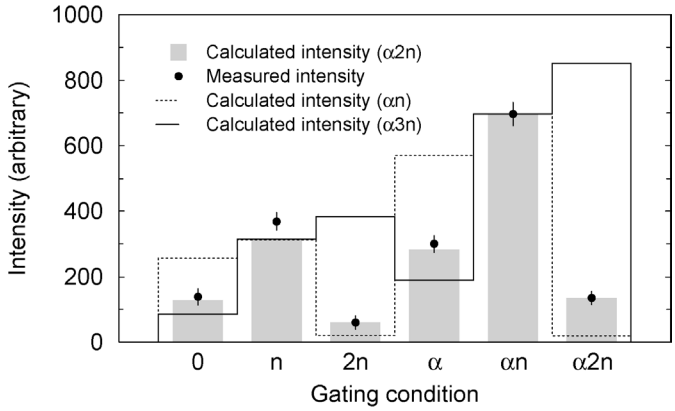

Fig. 1. Intensities of transitions in the various particle-gated matrices. The gating condition for the matrix is given on the horizontal axis. The solid black circles show the experimentally measured intensities of the ^{122}Ce band, determined by gating on the 298-keV transition and measuring the intensity of the 437-keV transition in the resulting spectrum. The shaded histogram gives the expected intensities if the transitions belong to the $\alpha 2n$-evaporation channel, calculated using the measured particle-detection efficiencies. The dotted and solid lines show the expected intensities for gamma rays which belong to the αn or $\alpha 3n$ evaporation channels, respectively. The calculated intensities are normalized so that the αn intensity matches that which was measured.

by gating on the 298-keV transition and measuring the intensity of the 437-keV transition in the resulting spectrum. The measured intensities are shown on Fig. 1.

The intensities of gamma rays in each particle-gated matrix are dependent upon the number of particles evaporated, and the particle-detection efficiencies. Thus, the intensities expected for a particular reaction channel can be estimated using the measured particle detection efficiencies. The expected intensities for the αn, $\alpha 2n$, and $\alpha 3n$ evaporation channels are also shown on Fig. 1. The calculated intensities have been normalized so that the intensity in the αn-gated matrix matches the observed intensity. The shaded histogram gives the intensities expected if the gamma rays belong to the $\alpha 2n$ channel, that is, to ^{122}Ce. The dashed and solid lines give the expected intensities if the gamma rays belong to the αn or $\alpha 3n$ channels, respectively. As mentioned above, gamma rays from the channels involving the evaporation of n neutrons are also observed in spectra gated on $(n+1)$ neutrons because of scattering between detectors; the magnitude of this effect for the gamma rays in the αn channel was estimated by measuring the intensity of known gamma rays in the $2pn$ evaporation channel (^{125}Ce) in the $2p2n$-gated matrix. On Fig. 1, the measured relative intensities do not agree well with the relative intensities expected for the αn or $\alpha 3n$ channels, but are in excellent agreement with the expectations for the $\alpha 2n$ channel. It is, however, possible that the gamma rays are from an $\alpha 2n$ evaporation channel following a reaction with a target contaminant such as ^{66,67,68,70}Zn or ^{12}C. However, this can be discounted because in each case these reactions would lead to excited states in known nuclei. Also, such contaminants would lead to other more intense reaction products with large cross sections, which were not observed. This analysis conclusively demonstrates that the observed gamma rays are emitted from states populated in the ^{64}Zn(^{64}Zn, $\alpha 2n$)^{122}Ce reaction.

In order to study the excited states of ^{122}Ce further, the particle-gated matrices were analyzed, and a particle-gated cube was sorted. The cube was gated on the ($\alpha 2n$, αn or $2n$) reaction channels. Coincidence gates were set in the cube and matrices on the 136-, 298-, 437-, and 557-keV transitions. Spectra from the matrices had a higher peak-to-background ratio and were less contaminated than those from the cube, presumably because of the low gamma-ray fold associated with the weak $\alpha 2n$ channel. The $\alpha 2n$-gated matrix contained 8×10^5 counts, which is just 0.01% of the total data set; this illustrates the high degree of selectivity available with the particle-gating technique. The intensity of the band, compared to other reaction products, suggests that the cross section for the production of ^{122}Ce in this reaction is about 500 μb,

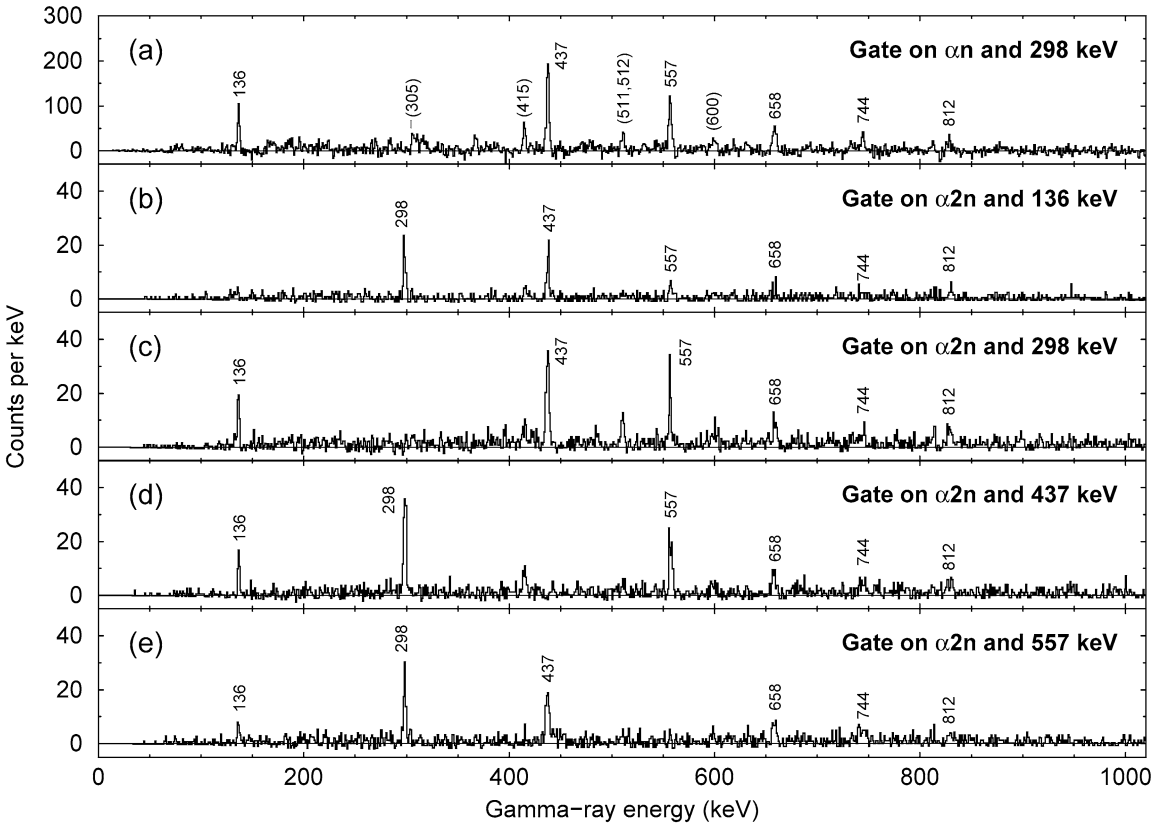

Fig. 2. Representative gamma-ray coincidence spectra taken from particle-gated matrices. The spectrum in panel (a) was taken from a matrix gated on the αn evaporation channel, and those in panels (b) to (e) were taken from a matrix gated on $\alpha 2n$. The gamma-ray transitions used as gates are given on the panels. The peaks are labelled with gamma-ray energies, given to the nearest keV, and all of the labelled peaks correspond to transitions in ^{122}Ce. The transitions in parentheses on panel (a) belong to nuclei produced in higher particle-multiplicity channels: 305 keV from ^{121}Ba ($\alpha 2pn$); 415 keV from ^{121}La ($\alpha p2n$); 512 keV from ^{119}Ba ($2\alpha n$); and 600 keV from ^{122}La (αpn). There is also be a contribution to the 511-keV peak from e^+e^- annihilation following β^+ decay.

which is in agreement with predictions from the code ALICE [14]. Representative spectra from the particle-gated matrices are given in Fig. 2. Panel (a) is a gate on the 298-keV gamma ray from the αn-gated matrix, and panels (b) to (e) are gates on the ^{122}Ce gamma rays from the $\alpha 2n$-gated matrix. The spectra all have very low background and feature only the transitions assigned to ^{122}Ce. Using gamma-ray intensities, energies, and coincidence relationships derived from the matrices, the level scheme proposed in Fig. 3 was deduced.

Angular-distribution measurements were used to help assign spins and parities to the excited states. The method used was a simple "two-point" angular distribution, as described in Ref. [21]; in this work, the spectra used were gated on the ($\alpha 2n$, αn or $2n$) evaporation channels. Gamma-ray intensities were measured in the detectors with θ close to 90° (28 detectors), and in the detectors with $129° < \theta < 163°$ (25 detectors). The ratios R of these intensities were taken and were found to have values close to 0.6 for stretched dipole transitions, and close to 1.1 for stretched quadrupole transitions. The method was calibrated by using transitions with established multipolarities in ^{122}La [19]. Using this method, multipolarity assignments can be made for all of the transitions identified in ^{122}Ce, including the tentative 812-keV transition. The measured ratios R are given in Table 1, along with values for four calibration transitions in ^{122}La. The values suggest that all of the transitions observed in ^{122}Ce have stretched

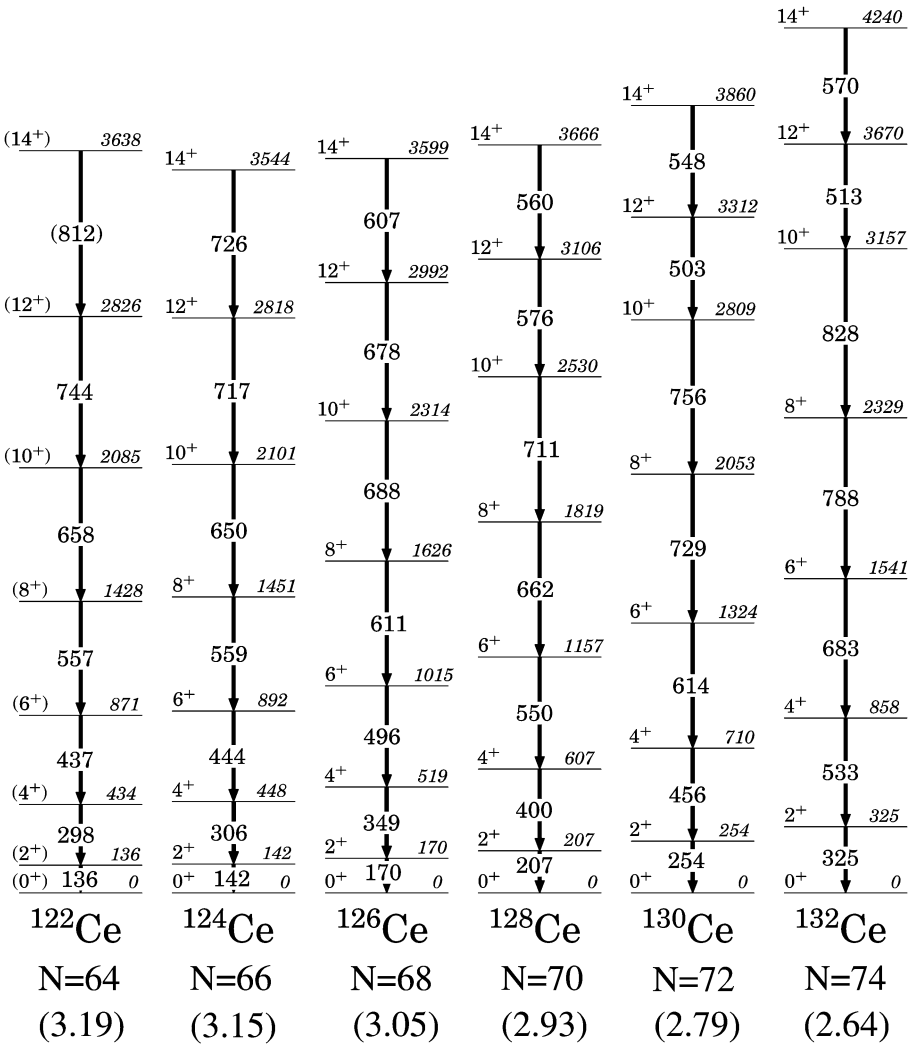

Fig. 3. Excitation-energy systematics of the ground-state rotational bands of the even–even cerium ($Z = 58$) isotopes with $122 \leqslant A \leqslant 132$, up to the 14^+ state. The excited states assigned to ^{122}Ce in this work are shown on the left. The data for $124 \leqslant A \leqslant 132$ are taken from Refs. [3,4,7–9]. The numbers in parentheses below each of the bands are the $E(4_1^+)/E(2_1^+)$ ratios.

E2 character; thus the ground-state rotational band extends to spin 12 $\hbar$, or tentatively 14 $\hbar$.

The systematics of the excitation energies in the ground-state rotational bands of the even–even cerium isotopes with $122 \leqslant A \leqslant 132$ are shown in Fig. 3, for the states up to ~ 4 MeV. Also given on the figure are the values of the $E(4_1^+)/E(2_1^+)$ ratios; these values show that the structure tends towards that of an axially-symmetric rigid rotor (3.33) with decreasing N. The value of $E(2_1^+)$ decreases with decreasing N, which suggests that the ground-state deformation increases.

An empirical relationship has been derived by Raman et al. [23] which relates the reduced transition probability $B(\mathrm{E2})$ to the value of $E(2_1^+)$ as

$$B\left(\mathrm{E2}\colon 0^+ \to 2^+\right) = 3.27 E\left(2_1^+\right)^{-1} Z^2 A^{-0.69} \left[(\mathrm{eb})^2\right], \quad (1)$$

where E is given in keV. This expression is considered to be superior to the well-known Grodzins' formula [24] because it is based on a larger data set and the parameters were derived from data in the Xe–Ba–Ce

Table 1
Properties of the gamma rays assigned to ^{122}Ce. The column labelled E_γ gives the gamma-ray energies, and that labelled I_γ gives the gamma-ray intensities. The column labelled R gives the angular-distribution ratios, as defined in the text. The column labelled "Mult" gives the assigned multipolarities of the transitions. The last four rows give transitions in ^{122}La which were used to "calibrate" the values of R

E_γ (keV)	I_γ	R	ΔI	$I_i^{\pi_i} \to I_f^{\pi_f}$	Mult
136.4(5)	100(7)	0.74(15)	2	$2^+ \to 0^+$	E2
298.3(5)	87(4)	1.15(28)	2	$4^+ \to 2^+$	E2
437.5(5)	83(4)	1.06(28)	2	$6^+ \to 4^+$	E2
556.5(5)	60(4)	1.11(18)	2	$8^+ \to 6^+$	E2
658(1)	43(4)	0.96(17)	2	$10^+ \to 8^+$	E2
744(1)	13(2)	1.22(23)	2	$12^+ \to 10^+$	E2
812(1)	5(2)	1.2(4)	2	$14^+ \to 12^+$	E2
231		1.14(11)	2	^{122}La	E2
560		1.16(9)	2	^{122}La	E2
149		0.70(6)	1	^{122}La	M1/E2
370		0.61(5)	1	^{122}La	M1/E2

region [25]; however, the differences in the extracted β_2 values are very small ($\sim 1\%$). The β_2 values are then determined using the expressions

$$Q_0 = \left[\left(\frac{16\pi}{5}\right)\frac{B(\mathrm{E2})}{e^2}\right]^{1/2} \tag{2}$$

and

$$\beta_2 = \left(\frac{5}{16\pi}\right)^{1/2}\left(\frac{4\pi Q_0}{3R^2 Ze^2}\right), \tag{3}$$

where $R = R_0 A^{1/3}$, and $R_0 = 1.2$ fm. Eq. (3) is discussed, for example, in Ref. [26]. The β_2 values extracted in this manner are presented in Fig. 4, as a function of N, for the even–even cerium isotopes with $122 \leqslant A \leqslant 132$.

The extracted β_2 values are compared to theoretical predictions in Fig. 4: the macroscopic-microscopic calculations of Möller, Nix, Myers, and Swiatecki (MNMS) [5]; the self-consistent Hartree–Fock–Bogoliubov (HFB) mean-field description by Duguet et al. [6]; and from total-Routhian surface (TRS) calculations, the method of which is discussed in Refs. [27,28]. The value of β_2 is predicted to peak at either $N = 64$ or $N = 62$. The TRS and MNMS calculations predict a maximum value of $\beta_2 \simeq 0.32$, but the HFB calculations predict a somewhat larger maximum of $\beta_2 \simeq 0.37$. For the lowest neutron numbers, the TRS and MNMS calculations underestimate the magnitude

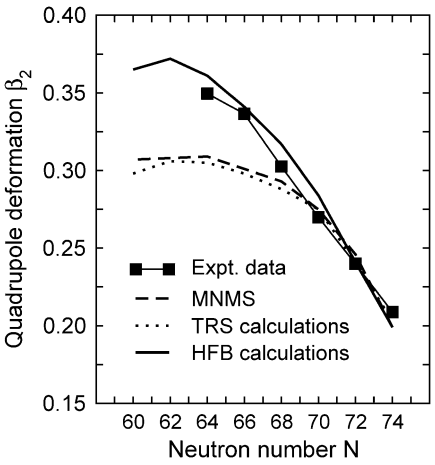

Fig. 4. Quadrupole deformation parameters β_2 of the even–even cerium ($Z = 58$) isotopes, plotted against neutron number N. The experimental values were extracted from the data using the expressions given in the text. The data for $124 \leqslant A \leqslant 132$ are taken from Refs. [3,4,7–9]. The experimental values are compared to the macroscopic–microscopic calculations of Möller, Nix, Myers, and Swiatecki (MNMS) [5], values from TRS calculations, and HFB self-consistent mean-field calculations [6].

of the deformations. However, the HFB calculations closely match the experimental values both in magnitude and in trend. For ^{122}Ce, the experimental data gives a value of $\beta_2 = 0.35$, compared to $\beta_2 = 0.36$ from the HFB calculations. Of the experimental values measured thus far, β_2 is largest for $N = 64$, although in the absence of data for $N = 62$ (^{120}Ce) it is not possible to state whether or not the maximum has been reached.

Woods–Saxon cranked-shell-model (CSM) calculations [29,30] have been performed for the even–even neutron-deficient cerium nuclei in order to predict the details of the quasiparticle alignments; specifically, their systematic dependence on N and β_2. Earlier work [3] has shown that the calculations reproduce the observed quasiparticle alignments reasonably well in the cerium nuclei. The calculations predict that pairs of both neutrons and protons from the $h_{11/2}$ sub-shell will align at rotational frequencies between 0.3 and 0.5 MeV/$\hbar$ in the even–even neutron-deficient cerium isotopes, and that the alignment frequencies depend on β_2 and N. As N decreases from 72 (^{130}Ce) to 64 (^{122}Ce), the frequencies of the $\pi(h_{11/2})^2$ alignments are predicted to increase from 0.3 to 0.4 MeV/$\hbar$. This range corresponds to a predicted increase in β_2

from 0.24 at $N = 72$ to 0.30 at $N = 64$. For these nuclei, the frequencies of the $\nu(h_{11/2})^2$ alignments are more complex, showing an oscillatory behavior around 0.4 to 0.45 MeV/$\hbar$, but generally occurring at least 0.05 MeV/$\hbar$ higher in frequency than the $\pi(h_{11/2})^2$ alignments. For ^{122}Ce, the dependence of the alignment frequencies on β_2 is shown in Fig. 5;

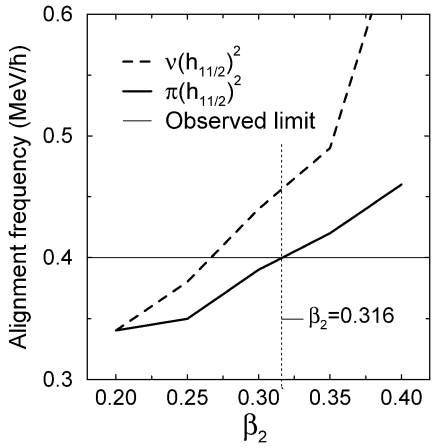

Fig. 5. Calculated alignment frequencies of the lowest pairs of $h_{11/2}$ neutrons (dashed line) and protons (solid line), as a function of the quadrupole deformation parameter β_2. The data are taken from Woods–Saxon cranking calculations, the method of which is described in Refs. [29,30]. The experimentally observed limit of rotational frequency (about 0.4 MeV/$\hbar$) is shown by a horizontal line.

the frequencies of both $\nu(h_{11/2})^2$ and $\pi(h_{11/2})^2$ alignments are calculated to increase with increasing β_2.

The experimentally-extracted aligned angular momenta I_x of the ground-state rotational bands of the $122 \leqslant A \leqslant 132$ cerium isotopes are plotted in Fig. 6 against rotational frequency. The aligned angular momentum for ^{122}Ce is shown on all of the panels, as a common reference. All of the cerium isotopes with $A \geqslant 124$ exhibit a clear rotational alignment between 0.3 and 0.4 MeV/$\hbar$. This alignment has previously been attributed to $h_{11/2}$ protons [3]. The observed frequency of this alignment increases with decreasing N, below $A = 130$, in agreement with the cranking calculations. The $\nu(h_{11/2})^2$ alignments are difficult to pinpoint, and are therefore difficult to compare [3], and are not discussed here.

In ^{122}Ce, the experimental data do not extend beyond 0.4 MeV/$\hbar$, so it is not possible to confirm the frequencies of the predicted $\pi(h_{11/2})^2$ and $\nu(h_{11/2})^2$ alignments. However, inspection of Fig. 5 shows that with $\beta_2 < 0.32$, the $\pi(h_{11/2})^2$ alignment would occur below 0.4 MeV/$\hbar$. There is no evidence for the onset of this alignment. Assuming that the trend in structure is continued by ^{122}Ce, the non-observation of the $\pi(h_{11/2})^2$ alignment thus places a lower limit on the deformation of $\beta_2 = 0.32$, a value consistent with the β_2 value inferred from $E(2_1^+)$, and with the theoretical calculations [5,6].

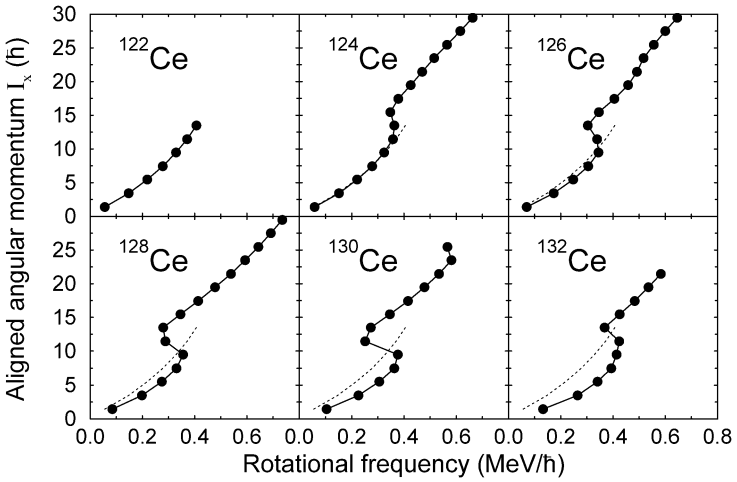

Fig. 6. Experimental aligned angular momenta I_x of the even–even cerium ($Z = 58$) isotopes with $122 \leqslant A \leqslant 132$, plotted against rotational frequency. The data for $124 \leqslant A \leqslant 132$ are taken from Refs. [3,4,7–9]. The data for ^{122}Ce are shown on each of the panels by a faint dashed line, as a common reference.

In summary, the very neutron-deficient ^{122}Ce nucleus has been identified for the first time, and excited states have been observed. This is the most neutron-deficient cerium isotope in which excited states have been identified to date. The excited states have been unambiguously assigned to ^{122}Ce by detecting gamma-ray transitions in coincidence with evaporated charged particles and neutrons. The spins of the states have been assigned on the basis of angular-distribution measurements. The states form a rotational band of stretched-quadrupole transitions extending up to 14 $\hbar$. The excitation energy of the 2_1^+ state suggests that ^{122}Ce is well deformed in its ground state, with $\beta_2 = 0.35$. Aligned angular momenta have been studied and compared to Woods–Saxon cranking calculations, and to the neighboring cerium isotopes. The $\pi(h_{11/2})^2$ alignment is not observed in ^{122}Ce until a rotational frequency of at least 0.4 MeV/$\hbar$, which suggests that the ground-state deformation has a lower limit of $\beta_2 = 0.32$. The value of β_2 deduced from $E(2_1^+)$ is consistent with this lower limit on β_2, and with theoretical predictions. The value of β_2 for ^{122}Ce continues the trend of increasing deformation with decreasing N. The deformations of the neutron-deficient cerium isotopes with $122 \leqslant A \leqslant 132$ are shown to be well reproduced by the HFB mean-field calculations of Ref. [6]. Calculations are underway [31] to investigate structure of the low-lying states in the cerium isotopes using the "beyond-mean-field model" described in Ref. [26]; it will be of considerable interest to compare the results of those calculations to the data obtained in the present work. Also, it will be very interesting to study the low-spin states of the $N = 62$ isotope ^{120}Ce in order to ascertain whether or not the trend of increasing deformation continues.

Acknowledgements

This work is supported in part by the NSF, the EPSRC (UK), and by the Department of Energy, Office of Nuclear Physics, under contract Nos. W-31-109-ENG-38 (ANL) and DE-FG02-88ER-40406 (Washington University).

References

[1] P.J. Woods, C.N. Davids, Annu. Rev. Nucl. Part. Sci. 47 (1997) 541.
[2] C.J. Lister, et al., Phys. Rev. Lett. 55 (1985) 810.
[3] J.F. Smith, et al., Phys. Rev. C 69 (2004) 034339.
[4] A.N. Wilson, et al., Phys. Rev. C 63 (2001) 054307.
[5] P. Möller, J.R. Nix, W.D. Myers, W.J. Swiatecki, At. Data Nucl. Data Tables 59 (1995) 185.
[6] T. Duguet, P. Bonche, P.-H. Heenen, J. Meyer, Phys. Rev. C 65 (2002) 014311.
[7] E.S. Paul, et al., Nucl. Phys. A 676 (2000) 32.
[8] D.M. Todd, R. Aryaeinejad, D.J.G. Love, A.H. Nelson, P.J. Nolan, P.J. Smith, P.J. Twin, J. Phys. G: Nucl. Phys. 10 (1984) 1407.
[9] E.S. Paul, et al., Nucl. Phys. A 619 (1997) 177.
[10] J.M. Nitschke, et al., Z. Phys. A 316 (1984) 249.
[11] G. Shanmugam, G.M.C. Vigila Bai, B. Kamalaharan, Phys. Rev. C 51 (1995) 2616.
[12] S. Kumar, D. Bir, R.K. Gupta, Phys. Rev. C 51 (1995) 1762.
[13] P.J. Nolan, F.A. Beck, D.B. Fossan, Annu. Rev. Nucl. Part. Sci. 44 (1994) 561.
[14] F. Plasil, M. Blann, Phys. Rev. C 11 (1975) 508.
[15] D.G. Sarantites, et al., Nucl. Instrum. Methods Phys. Res. A 530 (2004) 473.
[16] D.G. Sarantites, P.-F. Hua, M. Devlin, L.G. Sobotka, J. Elson, J.T. Hood, D.R. LaFosse, J.E. Sarantites, M.R. Maier, Nucl. Instrum. Methods Phys. Res. A 381 (1996) 418.
[17] C.N. Davids, et al., Nucl. Instrum. Methods Phys. Res. B 70 (1992) 358.
[18] D.C. Radford, Nucl. Instrum. Methods Phys. Res. A 361 (1995) 297.
[19] A.M. Fletcher, PhD thesis, University of Manchester, 2003.
[20] J.F. Smith, et al., in preparation.
[21] J.F. Smith, et al., Phys. Rev. C 61 (2000) 044329.
[22] J.F. Smith, et al., Phys. Lett. B 523 (2001) 13.
[23] S. Raman, J.A. Sheikh, K.H. Bhatt, Phys. Rev. C 52 (1995) 1380.
[24] L. Grodzins, Phys. Lett. 2 (1962) 88.
[25] S. Raman, C.W. Nestor Jr., S. Kahane, K.H. Bhatt, Phys. Rev. C 43 (1991) 556.
[26] M. Bender, H. Flocard, P.-H. Heenen, Phys. Rev. C 68 (2003) 044321.
[27] R. Wyss, J. Nyberg, A. Johnson, R. Bengtsson, W. Nazarewicz, Phys. Lett. B 215 (1988) 211.
[28] W. Nazarewicz, G.A. Leander, A. Johnson, Nucl. Phys. A 503 (1989) 285.
[29] W. Nazarewicz, J. Dudek, R. Bengtsson, I. Ragnarsson, Nucl. Phys. A 435 (1985) 397.
[30] S. Cwiok, J. Dudek, W. Nazarewicz, W. Skalski, T. Werner, Comput. Phys. Commun. 46 (1987) 379.
[31] P.-H. Heenen, M. Bender, in preparation.